Transient analysis of electrolyte-gated organic field effect transistors

Deyu Tu[a], Loïg Kergoat[b], Xavier Crispin[b], Magnus Berggren[b], Robert Forchheimer[a]
[a]Information Coding, ISY Linköping University, SE-581 83 Linköping Sweden
[b]Organic Electronics, ITN Linköping University, SE-601 74 Norrköping Sweden

ABSTRACT

A terminal charge and capacitance model is developed for transient behavior simulation of electrolyte-gated organic field effect transistors (EGOFETs). Based on the Ward-Dutton partition scheme, the charge and capacitance model is derived from our drain current model reported previously. The transient drain current is expressed as the sum of the initial drain current and the charging current, which is written as the product of the partial differential of the terminal charges with respect to the terminal voltages and the differential of the terminal voltages upon time. The validity for this model is verified by experimental measurements.

Keywords: Charge model, electrolyte, field effect transistors, simulation, transient

1. INTRODUCTION

Organic field effect transistors (OFETs) are intensively explored as one of most important basic blocks in organic electronics due to their potential applications in flexible, low-cost, and large-area electronic circuits.[1-3] Using organic field effect transistors, both digital and analog circuits have been demonstrated, such as inverters, logic gates, ring oscillators, etc.[4-8] Even more, some advanced circuits at large-scale have been implemented with organic transistors, for instance, radio-frequency identification (RFID) tags and analog-digital converters (ADC).[9-10] To realize complex circuit functions with organic field effect transistors, the complexity of large-scale circuits requires accurate modeling of the transistors. Different from conventional silicon metal-oxide-semiconductor field effect transistors (MOSFETs), OFETs usually are operated in accumulation mode. Numerous models have been developed for OFETs based on the possible mechanisms of charge transport within organic semiconductors.[11-15] There are two main mechanisms widely accepted: variable range hopping[11] and tail-distributed traps.[12] However, most of the models for OFETs are devoted to deal with the dc behaviors.[11-15] Only a few examples discuss the transient behaviors of OFETs.[16-18]

In this work, we report a terminal charge and capacitance model for transient analysis of electrolyte-gated organic field effect transistors (EGOFETs). EGOFETs are organic field effect transistors, which, instead of using insulating materials as gate dielectric layer, like in, conventional OFETs, use an electrolyte. By applying a bias, the ions in the electrolyte form electrical double layers at the metal-electrolyte and at the electrolyte-semiconductor interface, providing a huge capacitance per unit area. The EGOFETs benefit from this huge capacitance, exhibiting very low operation voltage. Our previous work[19] has reported a drain current model for EGOFETs, based on charge drift transport, taking voltage-dependent electrical-double-layer capacitance, contact effect and short-channel effect into account. From this drain current model, a charge and capacitance model is derived based on the Ward-Dutton partition scheme.[20] The terminal charges are written as an expression including terminal voltages and other model parameters from the previous work,[19] while the self-capacitances and transcapacitances are expressed as the partial derivatives of the charges with respect to the terminal potentials. The channel transit time is obtained from the channel charge and the channel current. The transient current is the sum of the initial current and the charging current. The charging current is then derived from the product of the partial differential of the terminal charges with respect to the terminal voltages and the differential of the terminal voltages upon time. The validity for this model is verified by experiments and the limits are discussed as well. The transient model is of special interest for simulation of integrated circuits implemented by EGOFETs.

2. MODEL DERIVATION

The drain current expressions of our previous work[19] were deduced assuming dc operation. Eq. (1) presents the drain current in the linear regime as

Organic Field-Effect Transistors XI, edited by Zhenan Bao, Iain McCulloch, Proc. of SPIE Vol. 8478
84780L · © 2012 SPIE · CCC code: 0277-786/12/$18 · doi: 10.1117/12.929886

$$I_D = \frac{W}{L}\mu_0[C_0\frac{{V_{GT}}^{\gamma+2}-(V_{GT}-V_D)^{\gamma+2}}{\gamma+2}+C_v\frac{{V_{GT}}^{\gamma+\chi+2}-(V_{GT}-V_D)^{\gamma+\chi+2}}{\gamma+\chi+2}], \quad (1)$$

where W is the channel width, L is the channel length, μ_0 is the low-field mobility, C_0 is the voltage-independent capacitance, C_v is the voltage-dependent capacitance, V_{GT} is the gate voltage V_G minus the threshold voltage V_T, V_D is the drain voltage, γ is the mobility enhancement factor, and χ is the electric double layer capacitance (EDLC) voltage-dependent factor.

However, the terminal voltages applied to the transistor usually vary over time. Consequently, the charges stored at device terminals vary as charging currents flow into/out the terminals. Here, we analyze the varying terminal charges and derive the transcapacitances, the transit time and the transient drain current for EGOFETs, based on a terminal charge and capacitance model. For this model, we only consider the intrinsic transistor, which includes only the channel area where the field effect takes place.

2.1 Terminal Charges

Generally, EGOFETs are operated as three-terminal devices, where voltages are applied to source, drain, and gate electrodes. The charges associated with each terminal have to be considered here. The gate charge Q_G is calculated by integrating the accumulated charge along the channel, thus

$$Q_G = -W\int_0^L Q(x)dx, \quad (2)$$

where $Q(x)$ is the accumulated charge at position x in the channel, $0<x<L$.

According to the Ward-Dutton linear partition scheme,[20] the drain charge Q_D can be computed as

$$Q_D = W\int_0^L \frac{x}{L}Q(x)dx. \quad (3)$$

Then, the source charge Q_S is equal to the minus sum of Q_G and Q_D due to the charge conservation, as follow

$$Q_S = -(Q_G + Q_D). \quad (4)$$

Considering the voltage-dependent EDLC in EGOFETs, we have $Q(x)$ as

$$Q(x) = C_0(V_{GT}-V(x)) + C_v(V_{GT}-V(x))^{\chi+1}. \quad (5)$$

From the dc drain current model,[19] the channel current at point x per unit width (I_D/W) is given by $I_D/W=\mu(x)Q(x)|E(x)|$, where $\mu(x)$ is the voltage-dependent charge mobility and $E(x)$ is the electric field given by the drain voltage along the channel, at point x in the channel. The mobility $\mu(x)$ is related to the voltage potential at that location and can be written as $\mu(x)=\mu_0(V_{GT}-V(x))^{\gamma}$ ($\gamma>0$) and $E(x)=\partial V(x)/\partial x$. The partial along the channel dx can then be written as

$$dx = \frac{\mu(x)WQ(x)}{I_D}dV(x). \quad (6)$$

Integrating Eq. (6), we obtain x

$$x = \frac{W}{I_D}\int_0^{V(x)}\mu(x)Q(x)dV(x)$$
$$= \frac{\mu_0 W}{I_D}\left[\frac{C_0\left(V_{GT}^{\gamma+2}-\left(V_{GT}-V(x)\right)^{\gamma+2}\right)}{\gamma+2}+\frac{C_v\left(V_{GT}^{\gamma+\chi+2}-\left(V_{GT}-V(x)\right)^{\gamma+\chi+2}\right)}{\gamma+\chi+2}\right]. \quad (7)$$

Substituting Eq. (5) and (6) into Eq. (2), the gate charge Q_G is derived as

$$Q_G = -W\int_0^L Q(x)dx = -\frac{\mu_0 W^2}{I_D}\int_0^{V_D}\left(V_{GT}-V(x)\right)^{\gamma}\left(C_0\left(V_{GT}-V(x)\right)+C_v\left(V_{GT}-V(x)\right)^{\chi+1}\right)^2 dV(x)$$

$$= -\frac{\mu_0 W^2}{I_D}\left[\begin{array}{l}\dfrac{C_0^2\left(V_{GT}^{\gamma+3}-\left(V_{GT}-V_D\right)^{\gamma+3}\right)}{\gamma+3}+\dfrac{2C_0C_v\left(V_{GT}^{\gamma+\chi+3}-\left(V_{GT}-V_D\right)^{\gamma+\chi+3}\right)}{\gamma+\chi+3}+\\ \dfrac{C_v^2\left(V_{GT}^{\gamma+2\chi+3}-\left(V_{GT}-V_D\right)^{\gamma+2\chi+3}\right)}{\gamma+2\chi+3}\end{array}\right] . \quad (8)$$

Similarly, by substituting Eq. (5), (6) and (7) into Eq. (3), the drain charge Q_D can be written as,

$$Q_D = \frac{W}{L}\int_0^L xQ(x)dx = \frac{\mu_0^2 W^3}{I_D^2 L}\sum_{i=1}^{7} f_i(V_G, V_D) , \quad (9)$$

where $f_i(V_G, V_D)$ (i=1,2…7) are results of the integration, as follows

$$f_1 = \left(\frac{C_0^3 V_{GT}^{\gamma+2}}{\gamma+2}+\frac{C_0^2 C_v V_{GT}^{\gamma+\chi+2}}{\gamma+\chi+2}\right)\frac{V_{GT}^{\gamma+3}-\left(V_{GT}-V_D\right)^{\gamma+3}}{\gamma+3}$$

$$f_2 = \left(\frac{2C_0^2 C_v V_{GT}^{\gamma+2}}{\gamma+2}+\frac{2C_0 C_v^2 V_{GT}^{\gamma+\chi+2}}{\gamma+\chi+2}\right)\frac{V_{GT}^{\gamma+\chi+3}-\left(V_{GT}-V_D\right)^{\gamma+\chi+3}}{\gamma+\chi+3}$$

$$f_3 = \left(\frac{C_0 C_v^2 V_{GT}^{\gamma+2}}{\gamma+2}+\frac{C_0^2 C_v V_{GT}^{\gamma+\chi+2}}{\gamma+\chi+2}\right)\frac{V_{GT}^{\gamma+2\chi+3}-\left(V_{GT}-V_D\right)^{\gamma+2\chi+3}}{\gamma+2\chi+3}$$

$$f_4 = -\frac{C_0^3}{\gamma+2}\frac{V_{GT}^{2\gamma+5}-\left(V_{GT}-V_D\right)^{2\gamma+5}}{2\gamma+5}$$

$$f_5 = -\left(\frac{2C_0^2 C_v}{\gamma+2}+\frac{C_0^2 C_v}{\gamma+\chi+2}\right)\frac{V_{GT}^{2\gamma+\chi+5}-\left(V_{GT}-V_D\right)^{2\gamma+\chi+5}}{2\gamma+\chi+5}$$

$$f_6 = -\left(\frac{C_0 C_v^2}{\gamma+2}+\frac{2C_0 C_v^2}{\gamma+\chi+2}\right)\frac{V_{GT}^{2\gamma+2\chi+5}-\left(V_{GT}-V_D\right)^{2\gamma+2\chi+5}}{2\gamma+2\chi+5}$$

$$f_7 = -\frac{C_v^3}{\gamma+\chi+2}\frac{V_{GT}^{2\gamma+3\chi+5}-\left(V_{GT}-V_D\right)^{2\gamma+3\chi+5}}{2\gamma+3\chi+5} . \quad (10)$$

The expressions for terminal charges can be used to derive the capacitance coefficients discussed below, including self-capacitance and transcapacitances.

2.2 Self-capacitances and Transcapacitances

Since we consider the intrinsic part of EGOFETs with three-terminal configuration, there are nine intrinsic capacitances defined as the partial derivatives of the charge at terminals with respect to the voltages,

$$C_{mn} = \pm \frac{\partial Q_m}{\partial V_n}, \tag{11}$$

where m and n denote the three terminals of transistors G, D, or S, and the positive sign applies only when m=n. Notice that the transcapacitances C_{mn} ($m \neq n$) are non-reciprocal, because the EGOFETs are active devices. Along with the self-capacitances C_{mn} (m=n), the transcapacitances can be written as the capacitive coefficients in a three-by-three matrix. This matrix reflects the dependency of charging currents on varying voltages, as

$$\begin{pmatrix} dQ_G/dt \\ dQ_D/dt \\ dQ_S/dt \end{pmatrix} = \begin{pmatrix} C_{gg} & -C_{gd} & -C_{gs} \\ -C_{dg} & C_{dd} & -C_{ds} \\ -C_{sg} & -C_{sd} & C_{ss} \end{pmatrix} \begin{pmatrix} dV_G/dt \\ dV_D/dt \\ dV_S/dt \end{pmatrix}. \tag{12}$$

Taking charge conservation into account, the relation between the self-capacitances and transcapacitances can be obtained as follows:[21]

$$\begin{aligned} C_{gg} &= C_{gs} + C_{gd} = C_{sg} + C_{dg} \\ C_{dd} &= C_{ds} + C_{dg} = C_{sd} + C_{gd} \\ C_{ss} &= C_{sg} + C_{sd} = C_{gs} + C_{ds} \end{aligned}. \tag{13}$$

From the above relationships, only four out of the nine capacitive coefficients are independent. Then, we derive four independent capacitances using Eq. (8) and (9), i.e.,

$$C_{gg} = \frac{\partial Q_G}{\partial V_G} = -\frac{\mu_0 W^2}{I_D}\left[\begin{aligned} &C_0^2\left(V_{GT}^{\gamma+2} - (V_{GT} - V_D)^{\gamma+2}\right) + 2C_0 C_v\left(V_{GT}^{\gamma+\chi+2} - (V_{GT} - V_D)^{\gamma+\chi+2}\right) \\ &+ C_v^2\left(V_{GT}^{\gamma+2\chi+2} - (V_{GT} - V_D)^{\gamma+2\chi+2}\right) \end{aligned}\right]$$

$$C_{dd} = \frac{\partial Q_D}{\partial V_D} = \frac{\mu_0^2 W^3}{I_D^2 L}\sum_{i=1}^{7}\frac{\partial f_i(V_G, V_D)}{\partial V_D}$$

$$C_{gd} = -\frac{\partial Q_G}{\partial V_D} = \frac{\mu_0 W^2}{I_D}\left[C_0^2(V_{GT} - V_D)^{\gamma+2} + 2C_0 C_v(V_{GT} - V_D)^{\gamma+\chi+2} + C_v^2(V_{GT} - V_D)^{\gamma+2\chi+2}\right]$$

$$C_{dg} = -\frac{\partial Q_D}{\partial V_G} = -\frac{\mu_0^2 W^3}{I_D^2 L}\sum_{i=1}^{7}\frac{\partial f_i(V_G, V_D)}{\partial V_G}. \tag{14}$$

The capacitance coefficients here can be used for both transient analysis and small-signal simulation of EGOFETs.

2.3 Transit time

The transit time is defined as the time it takes for charge carriers to flow across the channel. To calculate the transit time, the current along the channel is assumed to be constant, which is very common in dc modeling. For a channel element of length Δx, the transit time is given by $\Delta t = \Delta x / v_e$, where v_e is the velocity of charge carriers. Then, the transit time for the entire channel is

$$\tau = \int_0^L \frac{dx}{v_e} = -\frac{W}{I_D}\int_0^L Q(x)dx$$
$$= \frac{\mu_0 W^2}{I_D^2}\left[\begin{array}{c} \dfrac{C_0^2\left(V_{GT}^{\gamma+3} - \left(V_{GT}-V_D\right)^{\gamma+3}\right)}{\gamma+3} + \dfrac{2C_0C_v\left(V_{GT}^{\gamma+\chi+3} - \left(V_{GT}-V_D\right)^{\gamma+\chi+3}\right)}{\gamma+\chi+3} + \\ \dfrac{C_v^2\left(V_{GT}^{\gamma+2\chi+3} - \left(V_{GT}-V_D\right)^{\gamma+2\chi+3}\right)}{\gamma+2\chi+3} \end{array}\right]. \quad (15)$$

As an estimation of the charging time of the transistor channel, the transit time represents the intrinsic delay of the device.

2.4 Transient currents

In terms of the steady-state current and terminal charges, we can derive a simple expression for transient drain and source currents. Neglecting generation and recombination, the current-continuity equation[22] can be written as

$$W\frac{\partial Q(x,t)}{\partial t} = \frac{\partial I(x,t)}{\partial x}, \quad (16)$$

where $Q(x, t)$ is the time-varying charges and $I(x, t)$ is the time-varying channel current.

Integrating Eq. (16) from source to drain and substituting the initial currents that are equal to the steady channel current (e. g. Eq. (1)), we obtain the transient drain and source current:

$$i_D(t) = I_{D0}(t) + \frac{dQ_D}{dt}$$
$$i_S(t) = I_{S0}(t) - \frac{dQ_S}{dt}, \quad (17)$$

where $I_{D0}(t)$ and $I_{S0}(t)$ are the initial currents at drain and source, respectively.

From Eq. (12), the charging currents can be rewritten as

$$\frac{dQ_D}{dt} = -C_{dg}\frac{dV_G}{dt} + C_{dd}\frac{dV_D}{dt} - C_{ds}\frac{dV_S}{dt}$$
$$\frac{dQ_S}{dt} = -C_{sg}\frac{dV_G}{dt} + C_{sd}\frac{dV_D}{dt} - C_{ss}\frac{dV_S}{dt}. \quad (18)$$

Hence, the transient currents can be calculated with the capacitive coefficients and the dc currents, by substituting Eq. (18) into Eq. (17). Note that the source is usually grounded in practical measurements, which will simplify Eq. (18).

3. RESULTS AND DISCUSSION

To illustrate the aforementioned expressions, the dependence of the terminal charges on the gate/drain bias is graphed here, as well as the capacitance coefficients. The terminal charges and capacitance coefficients are interpreted in terms of operation regimes. The transit time with respect to the channel length or terminal bias is also presented. Finally, we discuss the dynamic drain/source currents associated with pulse bias at gate/drain and compare the model outcome with experimental data. The model parameters used here are inherited from the drain current model reported in the previous work,[19] where W=1000 μm, L =50.5 μm , V_T = −0.27 V, γ = 1.33, χ= 0.67, μ_0=0.028 cm^2/Vs, C_0=5 μF/cm^2, and C_v=1.5 μF/cm^2 at $|V_{GT}|$=1 V. Generally, all equations are given for n-channel OFETs in this dynamic model, as well as the previous dc model, to simplify the derivation. However, the EGOFETs measured in our experiments are usually p-channel devices, which means the polarity of voltages and currents should be reversed.

As functions of the terminal bias, the stored charges at gate, drain, and source are shown in Fig. 1. For a fixed $-V_D$=0.3V (p-channel transistors), the charges are plotted in function of $-V_G$, as shown in Fig. 1(a). At lower V_G, the channel is off, resulting in a low amount of charge. The accumulated gate charge increases continuously with ascending $-V_G$. The stored charge at the drain starts to drop as soon as V_G is high enough to open the channel. However, when $|V_G|<|V_D+V_T|$, which corresponds to the operation in the saturation regime, the charge begins to accumulate at drain and source again due to saturated charge transport. The trend will be reversed as soon as further increased $-V_G$ makes the device operating in the linear regime. In the opposite, the charges as $-V_D$ increased from 0.2 to 1 V are plotted in Fig. 1(b), by fixing $-V_G$=0.6V. From this figure, we also can observe the charge accumulation in the saturation regime.

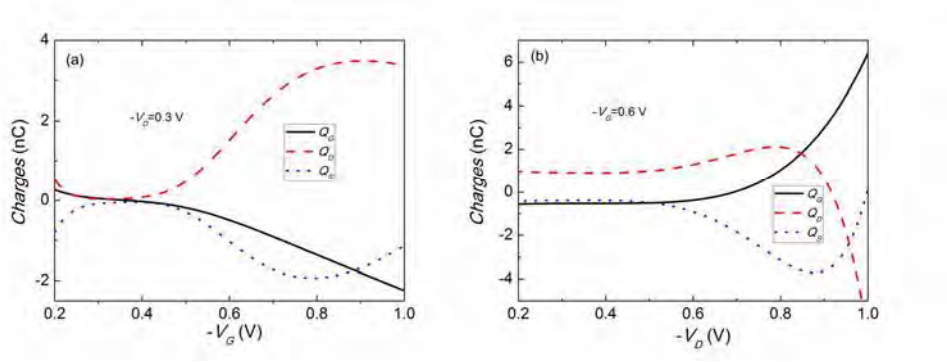

Figure 1. Terminal charges as a function of gate voltage (a) and drain voltage (b).

Taking the capacitances at the gate as example, we compare the capacitances calculated from the expressions above, presented in Fig. 2. Again, the drain voltage is fixed and the capacitances with respect to gate voltage are plotted in Fig. 2(a). For lower $-V_G$, the capacitances C_{gg} and C_{gd} are very small and C_{gs} is almost negligible due to the small amount of charge carriers in the channel. The C_{gg} and C_{gs} increase rapidly for higher $-V_G$, as the channel charge increases. But the C_{gd} remains negligible since the device operates in the saturation regime. For even higher $-V_G$, the transistor enters the linear regime and both the C_{gd} and C_{gs} increase. Fig. 2(b) presents the capacitance versus drain voltage at fixed gate voltage. C_{gs} is kept constant since the source is grounded and the V_G is fixed. C_{gg} and C_{gd} increase rapidly when the transistor operates in the saturation regime.

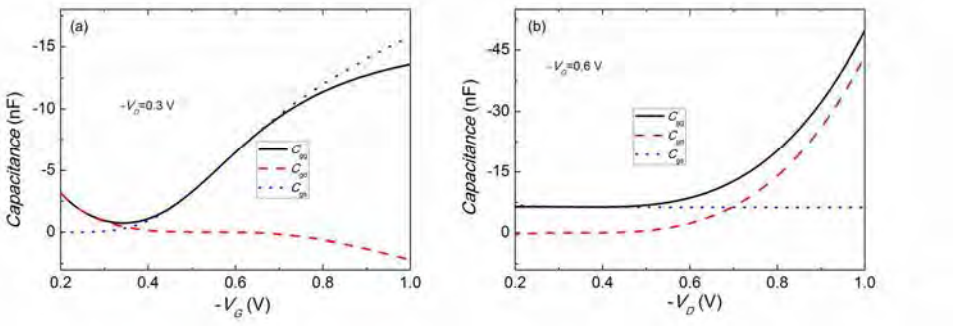

Figure 2. Self-capacitance and transcapacitances at the gate, as a function of gate voltage (a) and drain voltage (b).

The transit time τ with respect to V_{GT} and channel length L is shown in Fig. 3. As expected, the transit time is inversely proportional to $-V_{GT}$ (Fig. 3(a)) and proportional to the square of L (Fig. 3(b)). Increasing gate voltage can decrease the transit time for lower $-V_{GT}$, however, due to the velocity saturation, the affection of gate voltage on the transit time is almost negligible for higher $-V_{GT}$. Moreover, for very short channel length, the transit time of EGOFETs is not limited by charge transport in the channel but by electrolyte polarization,[23] which is not included in this work. For a transistor with L=50.5 μm, the transit time estimated by this model is around 1.3 ms, which is a reasonable value close to the measured results.[24]

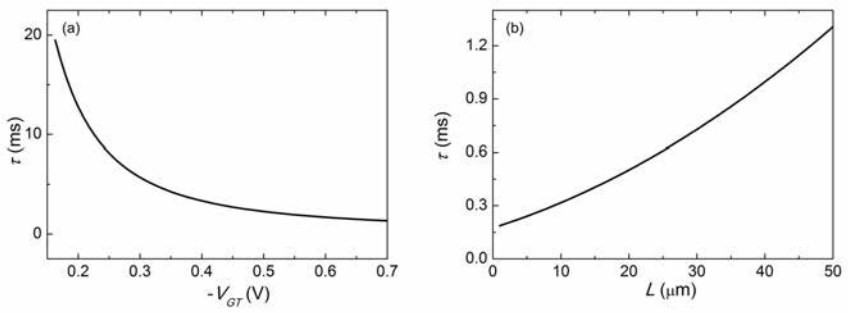

Figure 3. Transit time as a function of V_{GT} (a) and channel length L (b).

Finally, applying a voltage pulse to the gate, the transient response of currents at source and drain is presented in Fig. 4. The rise time t_r of the pulse has a significant effect on the charging current for the transient analysis. Fig. 4(a) presents a 1-V pulse with t_r=0.5 s >> τ=1.3 ms and the corresponding currents are shown in Fig. 4(b). When V_G reaches the threshold voltage V_T, electrons begin to flow from the source towards the drain. After a certain time, corresponding to the delay time t_d, electrons reach the drain and the conducting channel is completely formed. From Fig. 4(b), we can see the difference between the drain current i_D and the source current $-i_S$. In this case the charge currents at the beginning are usually small, thanks to t_r >> τ. When t_r is comparable to τ, the charge current gives a very sharp spike to the current waveform. Fig. 4(c) presents a 1-V pulse with t_r=10 ms and the corresponding currents are shown in Fig. 4(d). A very significant current spike can be observed as well as the clear delay of i_D. Here the static drain current is plotted as reference. For the experiment measurements (L=2 μm), we used a -1.2-V square pulse with t_r=4 μs (Fig. 4(e)). As expected, a very sharp charging current spike is observed in the drain current (Fig. 4(f)). The normalized i_D exhibits the same trend as the model predicts. Notice that the transition between transient current and steady current is smooth in the experimental data due to the inertia of electrons, which is not included here.

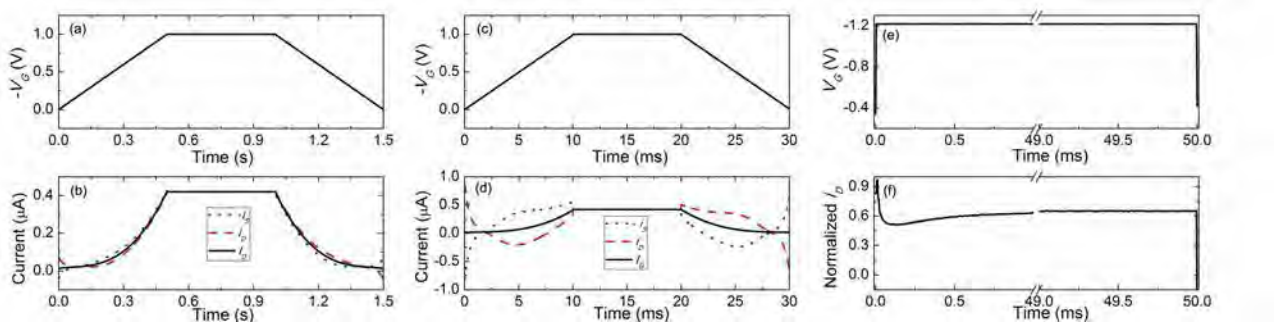

Figure 4. Pulse voltage waveforms at the gate (a)(c), and corresponding transient drain currents and negative source currents (b)(d) for t_r=0.5 s/10 ms, respectively. The steady drain currents are also shown in the simulation results (b)(d), while the measured drain current and gate voltage pulse are presented in (f)/(e) for t_r=4 μs.

4. CONCLUSION

In conclusion, this work presents a terminal charge and capacitance model for the transient analysis of EGOFETs, based on a charge-drift static current model. Considering the intrinsic part of the transistors, the terminal charges and capacitance coefficients are derived from the Ward-Dutton partition scheme. The transit time is written as an expression mainly relative to gate voltage and channel length. Summing the charging current and initial current, we obtain the transient current at the device terminals. The charging current is predominant in the transient current when the rise time of applied bias is comparable to the device transit time, which is observed in the experimental measurements as well. This charge and capacitance model is promising for circuit simulation which includes dynamic operations of EGOFETs.

ACKNOWLEDGMENT

The authors gratefully thank the Strategic Research Foundation SSF for financial support under the “OPEN” project.

REFERENCES

[1] Klauk, H., "Organic thin-film transistors," Chemical Society Reviews 39(7), 2643-2666 (2010).
[2] Sirringhaus, H., Tessler, N. and Friend, R. H., "Integrated optoelectronic devices based on conjugated polymers," Science 280(5370), 1741-1744 (1998).
[3] Dimitrakopoulos, C., Purushothaman, S., Kymissis, J., Callegari, A. and Shaw, J. M., "Low-voltage organic transistors on plastic comprising high dielectric constant gate insulators," Science 283(5403), 822-824 (1999).
[4] Klauk, H., Gundlach, D. J. and Jackson, T. N., "Fast Organic Thin Film Transistor Circuits," IEEE Electron Device Letters 20(6), 289-291 (1999).
[5] Sirringhaus, H., Kawase, T., Friend, R. H., Shimoda, T., Inbasekaran, M., Wu, W. and Woo, E. P., "High-resolution inkjet printing of all polymer transistor circuits," Science 290(5499), 2123-2126 (2000).
[6] Nilsson, D., Robinson, N., Berggren, M. and Forchheimer, R., "Electrochemical logic circuits," Adv. Mater. 17(3), 353-358 (2005).
[7] Zschieschang, U., Halik, M. and Klauk, H., "Microcontact-Printed Self-Assembled Monolayers as Ultrathin Gate Dielectrics in Organic Thin-Film Transistors and Complementary Circuits," Langmuir 24(5), 1665-1669(2008).
[8] Herlogsson, L., Cölle, M., Tierney, S., Crispin, X. and Berggren, M., "Low voltage ring oscillators based on polyelectrolyte-gated polymer thin-film transistors," Adv. Mater. 22(1), 72-76(2010).
[9] Cantatore, E., Geuns, T. C. T., Gelinck, G. H., van Veenendaal, E., Gruijthuijsen, A. F. A., Schrijnemakers, L., Drews, S. and de Leeuw, D. M., "A 13.56-MHz RFID system based on organic transponders," IEEE Journal of Solid-State Circuits 42(1), 84-92 (2007).
[10] Xiong, W., Guo, Y., Zschieschang, U., Klauk, H. and Murmann, B., "A 3-V, 6-Bit C-2C Digital-to-Analog Converter Using Complementary Organic Thin-Film Transistors on Glass," IEEE Journal of Solid-State Circuits 45(7), 1380-1388 (2010).
[11] Vissenberg, M. and Matters, M., "Theory of the field-effect mobility in amorphous organic transistors," Phys. Rev. B 57(20), 12964-12967 (1998).
[12] Shur, M., and Hack, M., "Physics of amorphous silicon based alloy field-effect transistors," J. Appl. Phys. 55(10), 3831-3842 (1984).
[13] Natali, D., Fumagalli, L. and Sampietro, M. "Modeling of organic thin film transistors: Effect of contact resistances," J. Appl. Phys. 101(1), 014501 (2007).
[14] Locci, S., Morana, M., Orgiu, E., Bonfiglio, A. and Lugli, P., "Modeling of short-channel effects in organic thin-film transistors," IEEE Trans. Electron Devices, 55(10), 2561-2567 (2008).
[15] Marinov, O., Deen, M. J., Zschieschang, U. and Klauk, H. "Organic thinfilm transistors: Part I—Compact DC modeling," IEEE Trans. Electron Devices 56(12), 2952-2961 (2009).
[16] Dunn, L., Basu, D., Wang, L. and Dodabalapur, A., "Organic field effect transistor mobility from transient response analysis," Appl. Phys. Lett. 88(6), 063507 (2006).
[17] Chang, H. -C., Ruden, P. P., Liang, Y. and Frisbie, C. D., "Transient effects controlling the charge carrier population of organic field effect transistor channels," J. Appl. Phys. 107(10), 104502 (2010).
[18] Bernards, D. A. and Malliaras, G. G., "Steady-state and transient behavior of organic electrochemical transistors," Adv. Funct. Mater. 17(17), 3538–3544 (2007).
[19] Tu, D., Herlogsson, L., Kergoat, L., Crispin, X., Berggren, M. and Forchheimer, R., "A Static Model for Electrolyte-Gated Organic Field-Effect Transistors," IEEE Trans. Electron Devices 58(10), 3574-3582 (2011).
[20] Ward, D. and Dutton, R., "A charge-oriented model for MOS transistor capacitances," IEEE J. Solid-State Circuits SSC-13(5), 703–708 (1978).
[21] Lu, H. and Taur, Y., "An analytic potential model for symmetric and asymmetric DG MOSFETs," IEEE Trans. Electron Devices 53(5), 1161–1168 (2006).
[22] Adler, R. B., Smith, A. C and Longini, R. L., [Introduction to Semiconductor Physics], John Wiley & Sons, New York, (1964).

[23] Herlogsson, L., Noh, Y. -Y., Zhao, N., Crispin, X., Sirringhaus, H., and Berggren, M., "Downscaling of organic field-effect transistors with a polyelectrolyte gate insulator," Adv. Mater. 20(24), 4708-4713 (2008).
[24] Larsson, O., Said, E., Berggren, M. and Crispin, X., "Insulator polarization mechanisms in polyelectrolyte-gated organic field-effect transistors," Adv. Funct. Mater. 19(20), 1-8 (2009).